BOLETIN DE LA SOCIEDAD ESPAÑOLA DE
Cerámica y Vidrio
www.elsevier.es/bsecv

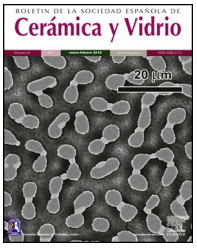

Crystallization characteristics and physico-chemical properties of glass–ceramics based on Li_2O–ZnO–SiO_2 system

*Saad M. Salman, Samia N. Salama, Hany A. Abo-Mosallam**

Glass Research Department, National Research Centre, 33 EL Bohouth St. (former EL Tahrir St.), Dokki, Giza, P.O. 12622, Egypt

ARTICLE INFO

Article history:
Received 16 November 2016
Accepted 18 February 2017
Available online 22 March 2017

Keywords:
Glass
Crystallization
Glass–ceramics
Thermal expansion
Durability

ABSTRACT

Glass materials based on lithium zinc silicate system of the composition $24Li_2O$–$20ZnO$–$56SiO_2$ LZS (mol%) were prepared and converted to glass–ceramics using controlled heat-treatment schedules. The LZS base glass system was modified by addition of Al_2O_3 and MO/ZnO replacements where MO = CaO, CdO and SrO oxides. Several crystalline phases were developed, including lithium zinc orthosilicate, α-quartz, β-spodumene solid solution, lithium meta and disilicate, Ca-wollastonite, Cd or Sr metasilicate, and Sr-zinc silicate of hardystonite type. The effects of crystallization process on some properties, like thermal expansion coefficient (TEC), chemical stability, and density of glass–ceramics were evaluated. The TEC of crystalline samples varied from 72×10^{-7} to 149×10^{-7} K^{-1}, 25–600 and density values in the range, 2.67–3.29 g/cm^3. The addition of Al_2O_3 and MO/ZnO replacements in the base glass led to improve the chemical durability of the glass–ceramics samples. As a result of the thermal and physico-chemical properties of the studied glass–ceramic, the materials acquire excellent properties and can be used to seal a variety of different metals and alloys.

Características de cristalización y propiedades físico-químicas de los materiales vitrocerámicos compuestos a base del sistema Li_2O-ZnO-SiO_2

Palabras clave:
Vidrio
Cristalización
Materiales vitrocerámicos
Expansión térmica
Durabilidad

RESUMEN

Los materiales de vidrio compuestos a base del sistema de silicato de cinc y de litio, de la composición $24Li_2O$–$20ZnO$-$56SiO_2$ LZS (mol %), se prepararon y se convirtieron en vitrocerámica con regímenes de tratamiento térmico controlado. El sistema de vidrio de base LZS se modificó mediante la adición de reemplazos de Al_2O_3 y MO/ZnO, donde MO = óxidos de CaO, CdO y SrO. Se desarrollaron varias fases cristalinas, incluyendo ortosilicato de cinc y de litio, de cuarzo α, solución sólida de espomudeno, metal litio y disilicato, Ca-wollastonita, metasilicato Cd o Sr, y silicato de cinc Sr de tipo hardistonita. Se evaluaron los efectos del

* *Corresponding author.*
E-mail addresses: ha.ebrahim@nrc.sci.eg, abomosallam@yahoo.com.au (H.A. Abo-Mosallam).
http://dx.doi.org/10.1016/j.bsecv.2017.02.002

proceso de cristalización en algunas propiedades, como el coeficiente de expansión térmica, la estabilidad química y la densidad de las vitrocerámicas. El coeficiente de expansión térmica de las muestras cristalinas varió de 72×10^{-7} a $149 \times 10^{-7}\,^{\circ}K^{-1}$ (25-600) y los valores de densidad en el intervalo 2,67-3,29 g/cm^3. La adición de reemplazos de Al_2O_3 y MO/ZnO en el vidrio base produjo una mejora de la durabilidad química de las muestras vitrocerámicas. Como resultado de las propiedades térmicas y físico-químicas de la vitrocerámica estudiada, los materiales adquieren excelentes propiedades y pueden utilizarse para sellar una variedad de diferentes metales y aleaciones.

Introduction

Glass–ceramics are promising materials for novel and smart applications. They are produced by controlling heat-treatment regime from the glass to obtain materials with unique properties in comparison with the basic glass [1]. Glass–ceramic materials possess a combination of interesting and useful properties like tunable thermal expansion coefficient (TEC), good mechanical and chemical durability as well as electrical resistivity, which lead to using it in different technological applications including seals and coatings [2]. Generally, there are various types of glass based on borate, phosphate, and silicate systems reported for the preparation of glass–ceramics reliable in metal sealing application. Glass–ceramics based on Li_2O–ZnO–SiO_2 (LZS) glass is one of the most promising systems characterized by a number of distinct features such as, excellent glass forming ability, high electrical resistivity, moderate sealing temperatures, wide range of thermal expansion coefficient, high fluidity and excellent wetting characteristics [3]. Therefore, glass–ceramic materials derived from a lithium zinc silicate system have an extensive applicability in sealing a variety of metals and alloys [4]. The thermo-physical and chemical property of the LZS glass–ceramics, mainly depends on the specific constituents of the original glass, heat treatment regime, type of the nucleating agent, and kind and amount of crystalline phase compositions. The crystallization characteristics and thermo-physical properties of (LZS) glass were studied by many authors [5–8]. $Li_2Si_2O_5$, Li_2SiO_3, $LiZnSiO_4$, and SiO_2 were developed as major phases in this type of glass–ceramic materials after the controlled heat-treatment is applied.

A series of studies to know the effect of adding Al_2O_3 on the crystalline phase constituents as well as properties of Li_2O–ZnO–SiO_2 system were reported for different glass compositions [9–11]. These glass–ceramics revealed considerable interest attributed to its adaptable thermal expansion coefficient, excellent hardness, good resistance to mechanical and thermal shock, and low chemical solubility [9–11]. The unique properties of the LZS glass–ceramics, mainly depend on the composition and the heat-treatment regime of glass. Alkali metal oxide [12] and alkaline earth oxide like magnesium oxide [13,14]; were added to the Li_2O–ZnO–SiO_2 glass system to study the effect of the change in the glass constituents on the crystalline phases formed and properties of resultant crystalized materials. Nevertheless, few researches about (LZS) glass–ceramics with CaO were performed [15,16]. To our knowledge, there is no available or rare research data about the role of CdO or SrO addition and their effect on the crystallization behavior and the physico-chemical properties of the Li_2O–ZnO–SiO_2 glassy system. So, the objective of this work is to study the influence of the addition of Al_2O_3 and the replacement of ZnO by CaO, CdO and SrO on the crystallization characteristics, including the nature and stability of the crystalline phases formed, the phase relation, microstructures, the chemical, and thermal properties of the glass–ceramic materials derived from the Li_2O–ZnO–SiO_2 system. The thermal expansion coefficient (TEC), density, and chemical durability properties of the obtained glass–ceramics were evaluated to investigate their efficiency to be used as a seal for a variety of different metals and alloys.

Experimental techniques

Glass composition and preparation

In the present work, eight glass samples based on the Li_2O–ZnO–SiO_2 system were investigated. The base glass with the composition $24Li_2O$–20ZnO–$56SiO_2$ (mole%) [17] was modified by adding (CaO, CdO, and SrO) at the expense of ZnO oxide. 0.1 mole% of Al_2O_3 oxide was also added to the base glass composition over 100 g glass oxides. The glasses were prepared by using reagents of lithium carbonate (Li_2CO_3), zinc oxide (ZnO), strontium carbonate ($SrCO_3$), calcium carbonate ($CaCO_3$), cadmium carbonate ($CdCO_3$), aluminum oxide (Al_2O_3), and quartz (SiO_2). The chemical nominal compositions of the investigated glass are summarized in Table 1. The well-mixed reagent powders were melted in a platinum crucible at a temperature range of 1350–1400 °C for 2 h to form homogenous molten glass, which was cast into a preheated stainless steel mold to form transparent glass by cooling rapidly. Then the cast glass samples were immediately transferred to an annealing furnace at about 450 °C and held at 3 h to reduce residual stress and then cooled to room temperature.

Differential thermal analysis (DTA)

The thermal behavior of the finely powdered (45–75 μm) glass samples was examined using the differential thermal analyzer (DTA, SDTQ 600–TA Instruments, USA) to determine the glass transition temperature (T_g) and crystal growth temperature (T_c) of the glass samples to obtain the optimum conditions for the heat-treatment regime. The DTA measurements were

Table 1 – The composition of the glasses studied.

Sample	Oxide nominal constitutions (mole%)						Oxide added mole
	Li_2O	ZnO	CaO	CdO	SrO	SiO_2	Al_2O_3
G_1	24	20	–	–	–	56	–
G_2	24	20	–	–	–	56	0.1
G_3	24	10	10	–	–	56	–
G_4	24	–	20	–	–	56	–
G_5	24	10	–	10	–	56	–
G_6	24	–	–	20	–	56	–
G_7	24	10	–	–	10	56	–
G_8	24	–	–	–	20	56	–

performed using about 30 mg of powdered samples that were placed in an alumina crucible. Measurements were made in the temperature range of 25–1000 °C, with a heating rate of 10 °C/min in a flowing high purity nitrogen environment.

Heat-treatment schedules

The glass–ceramic specimens, with minimum residual glassy phase without deformation, were obtained by the controlled crystallization of the glass using double stage heat-treatment regimes. The glasses were crystallized according to the DTA data in an electric muffle furnace provided with a temperature controller. At the endothermic peak temperature of each glass composition, the glass sample was soaked for 5 h, and then raised up to exothermic peak temperature recorded on the DTA of each glass for 10 h duration. After crystallization, the muffle furnace was switched off and the samples were allowed to cool down to room temperature.

X-ray diffraction analysis (XRD)

Identifications of the crystalline phases formed in the glass–ceramic specimens attributed to the controlled crystallization of the glasses were confirmed by X-ray diffraction analysis. X-ray diffraction (XRD) data were measured by (Panalytical, X Pert XPro, Netherlands) with Cu Kα radiation in the 2θ range from 5° to 70 at 0.02° steps, and JCPDF cards were used to identify the type of the crystalline phases formed.

Scanning electron microscope (SEM)

The microstructure characteristics of the crystallized specimens was carried out using a scanning electron microscope equipped with an energy dispersive spectrometer (SEM/EDS, Quanta FEG 250, Netherlands). For SEM characterization, freshly fractured surfaces crystallized specimens were etched by immersion in a (1%HF + 1% HNO_3) solution for 1 min. After that, the samples were washed with distilled water and dried in the dryer at 120 °C for 1 h. The fracture surfaces were coated with electro-conductive gold film for good conductivity by the sputtering method.

Thermal expansion coefficient

The thermal expansion coefficient (TEC) of the glass–ceramic materials was measured linearly from the thermal expansion curve, and was determined using a contact dilatometer, a thermal mechanical analyzer (Model: DIL-402PC, Netzsch, Germany) at a heating rate of 10 °C/min in the temperature range between 25 and 700 °C. The average linear TEC (α) of the bulk glass–ceramic rods of dimensions (20 mm × 5 mm × 5 mm) were calculated using the following equation:

$$\alpha = \frac{\Delta L}{L_0 \Delta T}$$

where ΔL, L_0, and ΔT are the linear expansion, the initial length of sample, and the specified temperature interval, respectively.

Density measurements

The bulk density of the glass–ceramics was measured at room temperature using the standard Archimedes' principle using distilled water as immersion liquid. Five different piece rods for each glass sample were used, free from bubbles and inclusions during the casting process. The relative weights of glass–ceramic samples in air and in distilled water were measured using an electrical digital balance with an accuracy of ±0.001 mg. The densities were calculated using the equation below:

$$\rho = \frac{\rho_w(T) W_s}{W_s - W_w}$$

where ρ is the sample density (g/cm^3), ρ_w (T) is the density of water at the measured temperature (g/cm^3),W_s is the sample weight in air (g) and W_w is the sample weight in water (g).

Chemical durability test

In the present work, the powder method was applied to assess the chemical durability of the glass–ceramic materials. The samples were crushed in an agate mortar and then sieved to obtain particles with diameter ranging between 0.63 and 0.32 mm [18,19]. Very fine grains can't be used because they will stick together and to the wall of the container and a large portion of the sample will therefore become shielded from the attack by aqueous solutions. The grains were then washed by decantation in ethyl alcohol three times and were then dried. The dried sample was accurately weighed (1 g) in a G4-sintered glass crucible, which was then placed in a 300 ml polyethylene beaker. The crystalline samples were tested for their chemical durability in 0.1 M HCl solution, 200 ml of the acidic solution was introduced into the polyethylene beaker. The polyethylene beaker with its contents was covered by polyethylene cover to reduce evaporation. The chemical durability

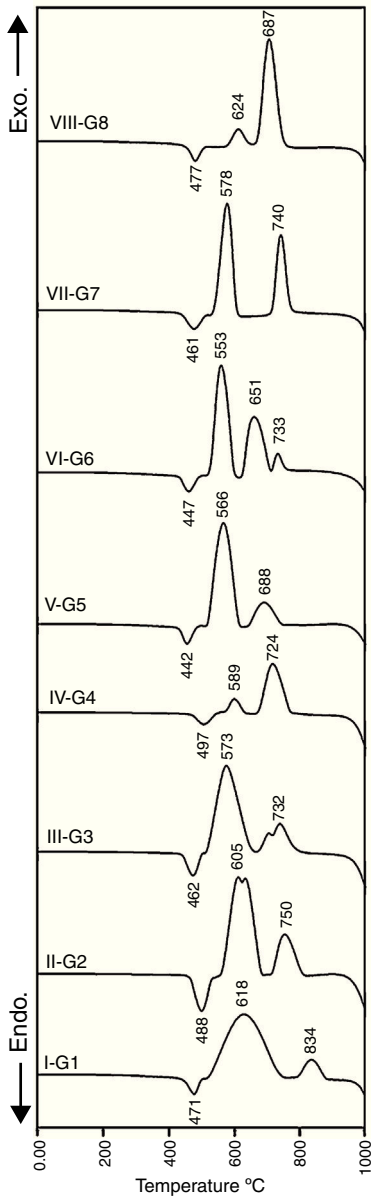

Fig. 1 – DTA curves of the investigated glasses.

was expressed as the weight loss percent. The experiments were carried out at 95 °C for 1 h to the different crystalline samples. The sintered glass crucible was then transferred and kept in an oven at 120 °C for 1 h, then transferred to cool in a desiccator. After cooling, the total weight loss percent of the samples were calculated.

Results and discussion

Crystallization behavior and microstructure

The crystallization process in the glasses is conventionally completed through a two-step heat-treatment regimes consisting of a nucleation stage followed by the crystal growth stage which is accurately determined by the DTA results. Fig. 1 represents the DTA plots of the investigated glasses at a heating rate of 10 °C/min. It is clear that all of the DTA curves have only one endothermic peak while various exothermic peaks, which referred to the crystal growth characteristics of the glasses, are also recorded. The onset of the endothermic peak which represents glass transition temperature (T_g) and temperature of an exothermic peak (T_c) were studied to determine the effect of the different addition and replacement processes in the base glass on the crystal phases formed. It is obvious from Fig. 1 that the base glass G_1 exhibits the transition temperature at around 471 °C, and two well-clear crystallization peaks T_{c1} and T_{c2} are around 618 °C and 834 °C respectively. The results show that the transition temperature was increased with the addition of 0.1 mole Al_2O_3 over 100 g oxides in the base glass. This conduct can be due to the increase of the viscosity of the resultant glass melts, and rigidity of the glass network structure by the formation of tetrahedral (AlO_4) group. It is agreed that the glass transition temperature value increases with increasing the structural strength of glass [20,21].

The value and trend of T_g due to the MO/ZnO replacement ratio and the type of MO where MO is CaO, CdO and SrO oxides are shown in Fig. 1. Intermediate oxides may either reinforce the network or further loosen the network, but do not have the ability to form a glass on their own. For instance Al_2O_3, MgO and ZnO have a tendency to take part in the glass as a network former making it an intermediate oxide. Ren et al. [22] stated that zinc has a tendency to take part in the glass network because of the covalent character of the bond it forms with oxygen. DTA results show that at 50% ZnO substitution, i.e., 10% mol of CaO, CdO, and SrO, the glass transition temperature shift toward lower values, i.e. a lower energy is needed to induce nucleation in the glasses. This may be explained on the basis that calcium, cadmium, and strontium charge balanced the zinc entering the network of the glass, while lithium acting like a modifier is not involved in the charge balance process so a relatively disrupted network could be occurring. While at 100% ZnO substitution, the glass network structure containing only strong bond between oxygen's and silica with respect to Zn–O bond, could result in an increase in the T_g as more energy is required to break the bonds [23]. In fact, these results are fully similar also to magnesium results when existing as network former in the glasses [24].

X-ray diffraction analysis is a powerful instrument to identify the crystalline phases developed during the controlled heat-treatment regime. Figs. 2 and 3 show the powder XRD patterns of the glass–ceramic specimens heat-treated at the optimum nucleation and crystal growth temperatures. These patterns show differences in type and proportions of the crystalline phases formed after heat-treatment and all phases were identified with PDF files. The phases developed in the base glass sample i.e., G_1 of composition $24Li_2O–20ZnO–56SiO_2$ (mole%) heat-treated at 470 °C/5 h and 835 °C/10 h, were lithium zinc orth-silicate γ_0-Li_2ZnSiO_4 (PDF, card No. 15-0056), α-quartz SiO_2 (PDF, card No. 33-1161), and small amount of lithium di-silicate $Li_2Si_2O_5$ (PDF, card No. 40-0376) [Fig. 2a, pattern I, Table 2]. These results support those reported by Stewart and Buchi [17] who determined the phase relationship in the $Li_2O–ZnO–SiO_2$ glass system. At the beginning of crystallization the unstable lithium zinc silicate phase with a formula close to $Li_3Zn_{0.5}SiO_4$ was formed. However by

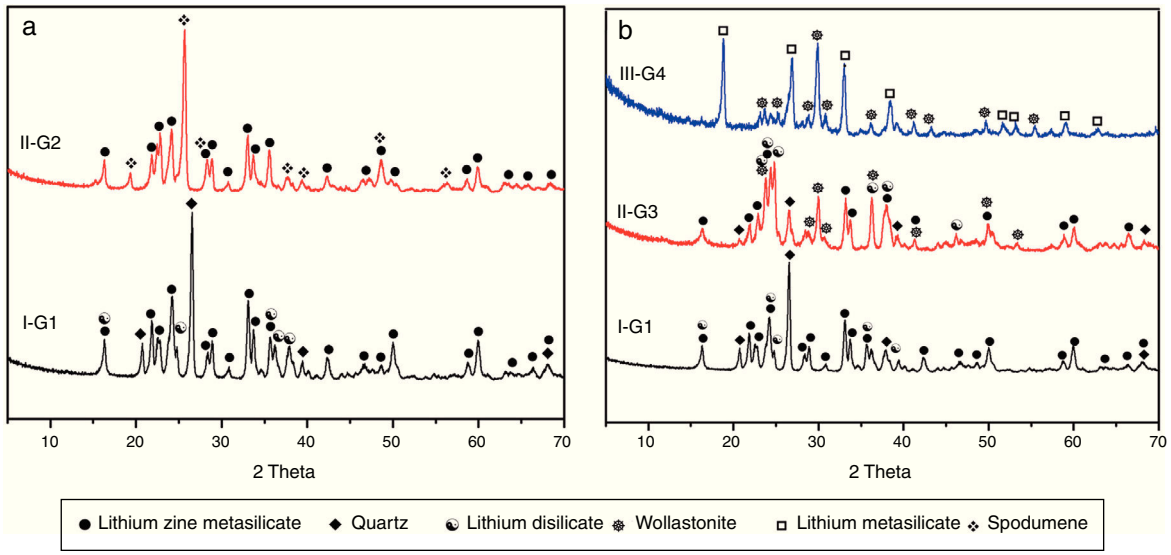

Fig. 2 – The X-ray diffraction patterns of the glass–ceramics samples for (a) effect of Al_2O_3 addition and (b) effect of CaO/ZnO replacement.

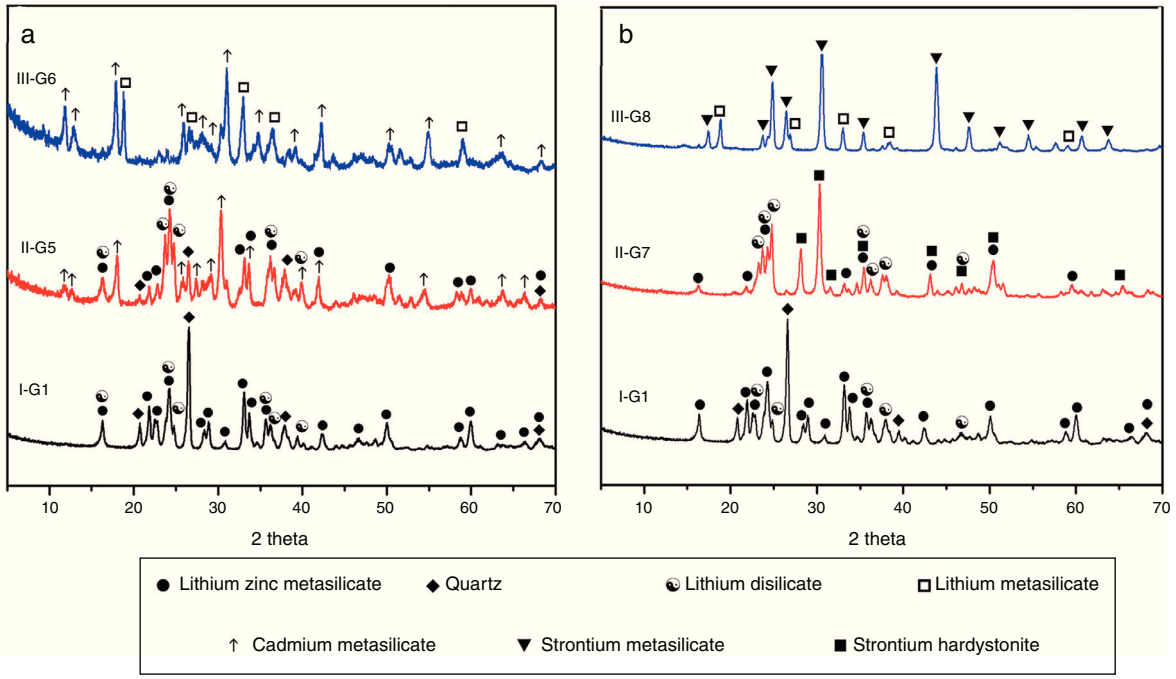

Fig. 3 – The X-ray diffraction patterns of the glass–ceramics samples for (a) effect of CdO/ZnO replacements and (b) effect of SrO/ZnO replacements.

Table 2 – Crystalline phases developed and propertied of the prepared glass–ceramics.

Sample	Crystalline phases developed	α (10^{-7} K^{-1}) (25–600 °C)	Density (g cm^{-3})	Weight loss % leaching by 0.1 N HCl
G_1	γ_0-Li_2ZnSiO_4, α-quartz, $Li_2Si_2O_5$	149	2.99	8.67
G_2	γ_0-Li_2ZnSiO_4, β-spodumene ss	89	2.93	6.43
G_3	γ_0-Li_2ZnSiO_4, α-quartz, $Li_2Si_2O_5$, $CaSiO_3$	112	2.81	6.57
G_4	Li_2SiO_3, $CaSiO_3$	72	2.67	2.68
G_5	γ_0-Li_2ZnSiO_4, α-quartz, $Li_2Si_2O_5$, $CdSiO_3$	121	3.25	7.01
G_6	Li_2SiO_3, $CdSiO_3$	80	3.29	4.12
G_7	γ_0-Li_2ZnSiO_4, $Li_2Si_2O_5$, $Sr_2ZnSi_2O_7$	102	2.95	8.01
G_8	Li_2SiO_3, $SrSiO_3$	79	2.91	5.78

increasing the degree and time of crystallization, the unstable $Li_3Zn_{0.5}SiO_4$ phase became more stable with a composition γ_0-Li_2ZnSiO_4 and remained in this form upon cooling to room temperature [10].

Generally the types and ratios of the resulting phases created in the crystallized glass specimens were significantly dependant on the diversity of the glass compositions and the controlled thermal treatment process. Mineralogically, γ0-Li_2ZnSiO_4 and β-spodumene solid solution (PDF, card No. 35-0797) phases were crystallized by the addition of 0.1 mole of Al_2O_3 on the base glass i.e., G_2, $Li_2Si_2O_5$ and α-quartz phases cannot be detected as confirmed from the XRD data [Fig. 2a, pattern II, Table 2]. It is suggested, therefore, that Al_2O_3 could be reacted with lithium di-silicate to form β-spodumene $LiAlSi_2O_6$ phase and the residual from alumina and lithium combined with silica to form spodumene phase as indicated in the following reaction:

$$\underset{\text{Lithium disilicate}}{Li_2Si_2O_5} + Al_2O_3 \rightarrow \underset{\text{β-spodumene}}{LiAlSi_2O_6} + \frac{1}{2}Al_2O_3 + \frac{1}{2}Li_2O \quad (1)$$

$$\frac{1}{2}Al_2O_3 + \frac{1}{2}Li_2O + \underset{\text{Silica}}{2SiO_2} \rightarrow \underset{\text{β-spodumene}}{LiAlSi_2O_6} \quad (2)$$

Theoretically, on the basis of petrochemical method [25], the recalculation of the resultant compositions into normative mineral molecules indicated that γ_0-Li_2ZnSiO_4, β-spodumene-$LiAlSi_2O_6$, and quartz-SiO_2 phases could be formed from the glass compositions. It is assumed therefore that the preferential formation of β-spodumene solid solution was favored by the great propensity of the pyroxene structure-spodumene to accommodate the SiO_2 component in its structure to form solid solution β-Spodumene ss phase. Salman et al. [26] proved leaving no room for doubt that β-spodumene is isostructural with silica polymorphs, β-quartz and keatite forming solid solution with silica SiO_2. In these glutted silica structure, AlO_4 tetrahedral replace the SiO_4 tetrahedral, mainly lithium and/or may be zinc, charge balance the aluminum entering the network of the glass structure.

Itemized study of the X-ray diffraction analysis was followed the effect of replaceming zinc oxide by calcium oxide in the base glass G_1 on the crystalline phases created in the glass–ceramic samples (G_3 and G_4) (Fig. 2b, Table 2). The controlled heat-treatment of glass G_3 (with CaO/ZnO equal 10 mole%) led up to the formation of γ_0-Li_2ZniO_4, $Li_2Si_2O_5$, α-quartz, and wollastonite $CaSiO_3$ (PDF, card No. 84-0655) phases. The wollastonite phase was formed partially at the expense of α-quartz phase, as indicated from XRD analysis (Fig. 2b, Pattern II). While, when the CaO/ZnO replacement reached up to 20 mole% i.e. G_4 lithium meat-silicate Li_2SiO_3 phase (PDF, card No. 83-1517) and wollastonite phase were formed (Fig. 2b pattern III). Glass–ceramic materials based on wollastonite $CaSiO_3$ have high potential and promising applications. These materials are used in biomedical applications for bone regeneration and magnetic hyperthermia therapy of bone defect and drug delivery [27]. Other recent applications of wollastonite based glass–ceramic materials include light-display and optoelectronic devices [28], as well as solid lubricant for ceramic molds [29].

Prolix study for the influence of CdO/ZnO replacement in the base glass on the crystalline phases formed of (G_5 and G_6) was detected by the XRD analysis (Fig. 3a, patterns II and III). The phases developed in the glass–ceramics sample G_5 with CdO/ZnO replacement equal to 10 mole were γ_0-Li_2ZniO_4, $Li_2Si_2O_5$, α-quartz and cadmium meta-silicate $CdSiO_3$ (PDF, card No. 35-0810). On further addition of CdO, i.e. sample G_6 (with 20 mole% CdO), the XRD analysis (Fig. 3a, Pattern III) revealed that only Li_2SiO_3 and $CdSiO_3$ phases were crystallized. Cadmium meta-silicate, $CdSiO_3$ phase is crystallized in the monoclinic space group which is isostructure with the structure of pseudo-wollastonite, $CaSiO_3$ [30]. Cadmium metasilicate based materials are promising for modern and smart applications. These materials show excellent phosphorescence property when doped with rare earth ions and some transition metal so can be used to tune the excitation energy storage and subsequent emission at room temperature [31].

The effect of adding strontium oxide instead of zinc oxide in the base glass with different ratios as 10 and 20 mole% (i.e. G_7 and G_8) (Fig. 3b, and Table 2) revealed that at low SrO/ZnO replacement equal 10 mole%, i.e. G_7, γ_0-Li_2ZnSiO_4, $Li_2Si_2O_5$ and strontium hardystonite $Sr_2ZnSi_2O_7$ (PDF, card No. 39-0235) phases were formed, as proved by the XRD (Fig. 3b, Pattern II). Strontium hardystonite compound belongs to a group of minerals known as melilite. This group has the general chemical formula $X_2T^1T^2{}_2A_7$, where X is a large mono-divalent or di-valent cation, T^1 and T^2 are small di- to tetravalent cations (T^1 = Be, Mg, Al, Co, Zn... T^2 = Al, Si, Ge ...), and A is an anion, frequently O, but also F or S [32]. The ceramic materials based on alkaline earth disilicate in the formula $A_2BSi_2O_7$ doped with rare earth ions become interesting in the field of photoluminescence because they have an excellent luminescent efficiency as well as high thermal and chemical stability [33]. Tiwari et al. [34] reported that during the crystallization of strontium zinc silicate glasses initially SiO_2 and $ZnSiO_3$ were crystallized as metastable phases. They postulated that by increasing the temperature and time of crystallization process the SiO_2 and $ZnSiO_3$ metastable phases are converted to more stable strontium zinc silicate of hardystonite type $Sr_2ZnSi_2O_7$ phase as illustrated from the following reaction.

$$ZnSiO_3(\text{orthorhombic}) + 2SrO(\text{glass}) + SiO_2(\text{glass}) \rightarrow Sr_2ZnSi_2O_7(\text{tetragonal}) \quad (3)$$

It should be noted that the increase of SrO instead of ZnO up to 20 mole%, (i.e. G_8) led to forming two crystalline phases Li_2SiO_3 and strontium meta-silicates $SrSiO_3$ (PDF, card No. 06-0415) as indicated from the XRD analysis (Fig. 3b, Pattern III). Strontium meta-silicates crystalline phase belongs to inosilicate mineral group with an Si:O ratio of 1:3 [35]. Thus, during the crystallization of glass G_8, it was assumed that SrO can combine with the equivalent amount of SiO_2 to form strontium meta silicates, according to the following reaction [34].

$$SiO_2(\text{hexagonal}) + SrO(\text{glass}) \rightarrow SrSiO_3(\text{monoclinic})/Sr_3Si_3O_9(\text{monoclinic}) \quad (4)$$

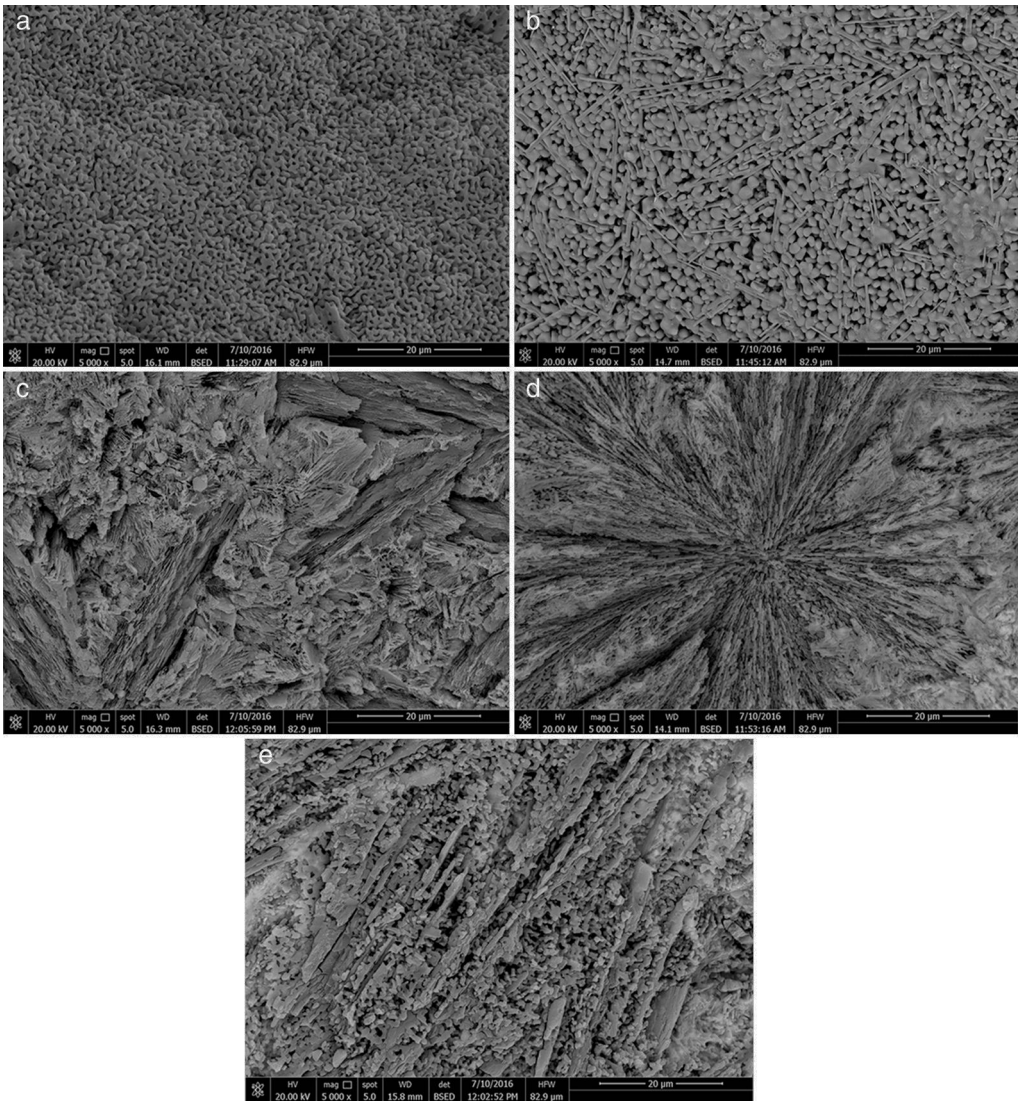

Fig. 4 – SEM micrographs of the glass–ceramics samples for (a) G_1, (b) G_2, (C) G_4, (d) G_6 and (e) G_8.

Microstructure not only plays a pivotal role in defining the final properties of glass–ceramics, but also is substantial to explain the conduct of controlled nucleation and crystallization processes, including the apportionment and morphology of crystals. In the glass–ceramic materials selecting the optimum composition and heat-treatment regime leads to form different microstructures, and hence different specific properties allowed these materials to be used in different technological applications. Fig. 4 shows the SEM micrographs of the glass–ceramic specimens prepared after controlling heat-treatment regime. Volume crystallization with rather fine microstructures was observed for all the compositions studied. Interconnected network microstructure of massive dendritic crystals was obtained from the base glass–ceramic specimen G_1 (Fig. 4a). This may be attributed to the crystallization of lithium zinc metasilicate crystals. Lu et al. [35] reported that the microstructure of Li_2ZnSiO_4 crystal phase form dendritic shape similar to Li_3PO_4 crystals. While, volume crystallization of typical spherical shape may be due to the formation of spodumene crystals developed in the sample G_2 as shown in (Fig. 4b). Hu et al. [36] found that β-quartz ss crystal phase forms network structure by a number of spherical crystals. The effect of CaO/ZnO, CdO/ZnO, and SrO/ZnO replacements on the grain microstructure behavior of the corresponding glass–ceramics appears by SEM micrographs in (Fig. 4c–e) respectively. The presence of CaO instead of ZnO in the base glass up to 20 mole% (i.e. G_4) enhanced the formation of volume fibrous crystals microstructure which characterized the wollastonite phase (Fig. 4c). Spherulite-like crystals were formed in the glass–ceramic sample G_6 with CdO/ZnO replacement ratio equal 20 mole%, (Fig. 4d). SEM micrograph of the fractured surface of G_8 (with 20 mole% SrO/ZnO replacement, Fig. 4e) revealed that volume crystallization of tiny aggregates microstructure was developed.

Physical properties

One of the main important advantages of glass–ceramics is that the chemical composition of the glass and the crystalline phases can be designed and controlled so, given the

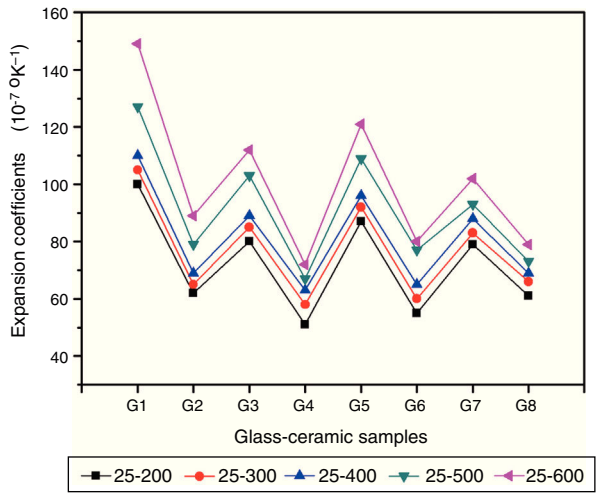

Fig. 5 – The coefficients of thermal expansion of the investigated glass–ceramics.

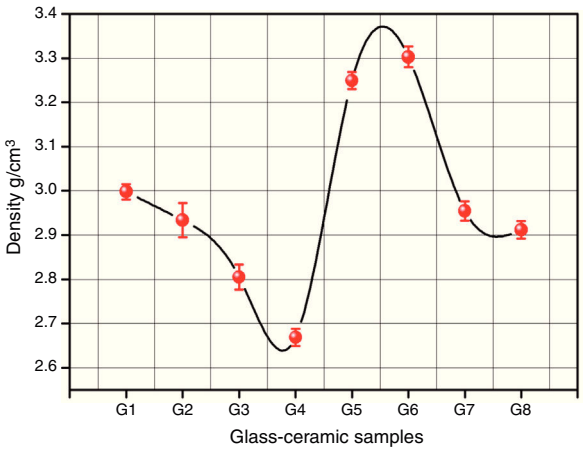

Fig. 6 – Density of the investigated glass–ceramics samples.

wonderful opportunity to control some physical properties like the thermal expansion coefficient. Fig. 5 shows the influence of the amount and kind of crystalline phases formed on the TECs of the investigated glass–ceramics. The average TEC values (25–600 °C) are represented in Table 2. It is known that, thermal expansion coefficient behavior of glass–ceramics basically depends on the amount and kind of the crystalline phases constituent and the proportion of the remaining glassy matrix between the crystals. As a matter of fact, the crystalline samples show moderate alpha values except that of the base sample G_1, which exhibits high values. The high α-values of the base glass–ceramic sample may be attributed to the presence of the high amount of γ_0-Li_2ZnSiO_4 phase, which have α-values $(110–180) \times 10^{-7}\,K^{-1}$ (25–1030 °C) [37]. The data obtained clearly revealed that the addition of Al_2O_3 in the base glass led to decreasing the α-values of the corresponding glass–ceramics i.e. G_2 as shown in Fig. 5. This may be due to the formation of much lower expansion coefficients β-spodumene ss phase instead of relatively high expanded lithium di-silicate and α-quartz phases. Lithium disilicate has α-value of $110 \times 10^{-7}\,K^{-1}$ (20–600 °C) [38] while spodumene and its solid solution have a low positive value $(3–9) \times 10^{-7}\,K^{-1}$ (20–700 °C) [39]. Demirkesen et al. [9] reported that the coefficient thermal expansion of the prepared glass–ceramics decreased from $12.4 \times 10^{-6}\,°C^{-1}$ to $6.3 \times 10^{-6}\,°C^{-1}$ with Al_2O_3/ZnO replacement in the Li_2O–ZnO–SiO_2 glass system. They, attribute the cause to the formation of low-expansion β-spodumene and its solid solutions phase instead of high-expansion cristobalite and γ0-LZS phases.

Detailed study for the effect of addition of CaO, CdO, and SrO instead of ZnO in the base glass on the thermal expansion coefficient created in the glass–ceramic specimens was detected (Fig. 5, Table 2). A progressive decrease in the α-values was observed with partial and complete CaO/ZnO replacements in the base glass samples i.e. G_3 and G_4. This is possibly due to the formation of the wollastonite phase, which has α-value of $(60–94) \times 10^{-7}\,K^{-1}$ [38] at the expense of relatively higher thermally expanding lithium zinc silicate and α-quartz phases. With respect to the effect of CdO/ZnO replacements in G_1 on the thermal expansion coefficients of the crystalline materials G_5 and G_6, it was seen that the addition of CdO instead of ZnO has also decreased the α-values of CdO-containing materials as shown in (Fig. 5, Table 2). This may be attributed to the formation of cadmium meta-silicate phase of lower expansion coefficient than that of γ_0-Li_2ZnSiO_4 and α-quartz phases. On the other hand, a decrease in the α-value of the SrO-containing samples was also detected. This may be due to the decrease or disappearance of lithium zinc metasilicate and α-quartz phases and appearance of relatively lower thermally expanding $Sr_2ZnSi_2O_7$ [40] and $SrSiO_3$ phases [41].

Bulk density of the glass–ceramic specimens is shown in Fig. 6 and Table 2. The data clearly indicates that the density values of the crystalline samples were in the range 2.67–3.29 g/cm³. Generally the density of glass–ceramic is significantly affected by the amount, density, and microstructure of crystalline phases formed in the materials. The microstructure containing large amounts of fracture and voids led to lower density values. The data recorded reveals that the addition of 0.1 mole Al_2O_3, CaO/ZnO, and SrO/ZnO replacements led to decreasing the density values of the crystalline glasses as compared with the base glass G_1. However, the density of the glass–ceramics was increased by the addition of CdO at the expense of ZnO in the base glass.

It can be explained the density differences in the glass–ceramic samples to the atomic weight diversity of elements which in turn is reflected on the molecular weight of the crystalline phases formed. So, the higher atomic weight of Cd element compared to that of Ca and Sr elements led to crystallization of the high molecular weight phase $CdSiO_3$ 188.49 in comparison with $CaSiO_3$ or $SrSiO_3$ phases with the molecular weight 116.16 and 163.70 respectively.

Chemical properties

The chemical durability is an important property of glass–ceramics and identifies dramatically their uses in different environments. It is predominantly agreed that the stability of glass–ceramics depends basically on the type and concentration of crystalline phases constituents, composition and amount of residual glassy matrix, and microstructure

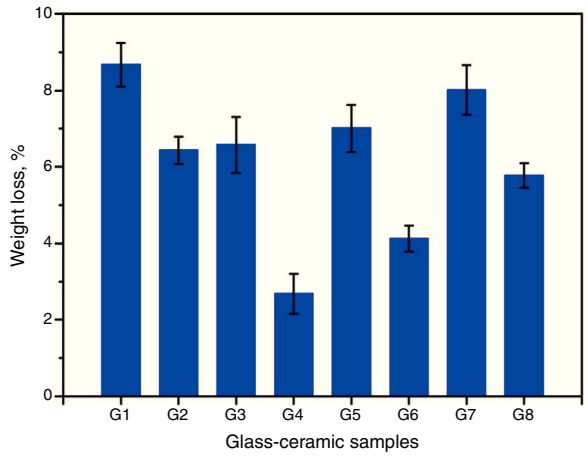

Fig. 7 – Chemical durability of the crystallized glasses in acidic media.

characteristics of the material, all of which is controlled by the glass batch design and the heat-treatment regime process [38]. The solubility of different crystalline phases in acidic media was studied by many researchers. Generally they reported that the response of phases toward acid attack can be classified into three different types, very resistant, weak resistivity, and decompose or gelatinize phases [32,38]. Fig. 7 shows the effect of the crystallization process on the chemical durability of the present glass–ceramic specimens. The results indicated that the chemical stability of the crystallized samples was significantly affected by the type and content of the crystalline phases formed in the materials. The addition of Al_2O_3 on the base glass, i.e., G_2 led to decreasing the leaching values of the crystalline glass as compared with that of the base glass–ceramic sample. This may be attributed to the crystallization of the high durable spodumene phase instead of the α-quartz and lithium di-silicate phases as indicated from XRD analysis Fig. 2a. The glass–ceramics based on lithium aluminosilicate phases like eucryptite, spodumene, and β-quartz solid solution have excellent chemical durability in different environments especially toward the acid attack [42,43].

Fig. 7 shows also the effect of CaO/ZnO, CdO/ZnO, and SrO/ZnO replacements with various ratios in the glasses on the chemical stability of the corresponding glass–ceramic materials. The present results revealed that all the different replacements in the base sample G_1 led to improving the chemical durability of corresponding glass–ceramic samples. This may be due to decrease or disappearance of the leachable lithium zinc meta-silicate Li_2ZnSiO_4 phase. Demirkesen and Göller [11] reported that the Li_2ZnSiO_4 phase decomposes easily by acid solution, and is responsible for the high weight losses occurred upon the leaching of glass–ceramic specimens. The results of the chemical stability indicated also that the samples G_7 and G_8 (with 10 and 20 mole% SrO) were less durable than the other examined samples containing CaO or CdO (Fig. 4). This may be due to that $SrSiO_3$ phase is less chemically resistant than $CaSiO_3$ and $CdSiO_3$ phases. Christoffersen et al. [44] reported that strontium (Sr) causes a crystal expansion due to the large atomic radius of Sr which increases the solubility of the mineral.

Summary and conclusions

The influence of crystallization characteristics of glasses based on the composition $24Li_2O–20ZnO–56SiO_2$ (mol%) on the crystalline phase formation, thermal, physical, and chemical properties of the prepared glass–ceramics was carefully studied. The base glass composition was modified by addition Al_2O_3 and replacement of ZnO by CaO, CdO and SrO oxides. The main crystalline phases formed were γ_0-Li_2ZnSiO_4, α-quartz, β-spodumene ss, $Li_2Si_2O_5$, Li_2SiO_3, $CaSiO_3$, $CdSiO_3$, $Sr_2ZnSi_2O_7$, and $SrSiO_3$. The TEC of crystalline samples varied from 72×10^{-7} to $149 \times 10^{-7}\,°K^{-1}$ (25–600); the density values were in the range, 2.67–3.29 g/cm^3 and the weight loss percent toward acid attack was between 2.68 and 8.67 wt%. The results of chemical durability show also that the addition of Al_2O_3 and MO/ZnO replacements in the base glass led to dramatic improvement in the glass–ceramics solubility. The physical and chemical properties of the developed glass–ceramic materials are suitable to be used as sealant materials with a variety of metals and alloys. Glass–ceramics material to-metal-sealing technology based on LZS system are widely used in electrical and electronic devices.

REFERENCES

[1] L. Karolina, C.K. Katarzyna, B.L. Maria, Thermal and spectroscopic characterization of glasses and glass–ceramics of $Li_2O–Al_2O_3–SiO_2$ (LAS) system, J. Mol. Struct. 1068 (2014) 275–282.
[2] G.P. Kothiyal, M. Goswami, B. Tiwari, K. Sharma, A. Ananthanarayanan, L. Montagne, Some recent studies on glass/glass–ceramics for use as sealants with special emphasis for high temperature applications, J. Adv. Ceram. 1 (2012) 110–129.
[3] P.W. McMillan, S.V. Phillips, G. Partridge, The structure and properties of a lithium zinc silicate glass–ceramic, J. Mater. Sci. 1 (1966) 269–279.
[4] M. Goswami, P. Sengupta, K. Sharma, R. Kumar, V.K. Shrikhande, J.M.F. Ferreira, G.P. Kothiyal, Crystallization behaviour of $Li_2O–ZnO–SiO_2$ glass–ceramics system, Ceram. Int. 33 (2007) 863–867.
[5] R. Morell, K.H.G. Ashbee, High temperature creep of lithium zinc silicate glass–ceramics. Part 2. Compression creep recovery, J. Mater. Sci. 8 (1973) 1271–1277.
[6] R. Lyall, K.H.G. Ashbee, High temperature plasticity of lithium zinc silicate glass–ceramics. Part 1. Constant strain-rate tests, J. Mater. Sci. 9 (1974) 576–582.
[7] I.W. Donald, B.L. Metcalfe, A.E.P. Morris, Influence of transition metal oxide additions on the crystallization kinetics, microstructures and thermal expansion characteristics of a lithium zinc silicate glass, J. Mater. Sci. 27 (1992) 2979–2999.
[8] Y. Chen, W. Li, Y. Zhang, Z. Shen, D. Yang, X. Song, Crystallization and thermal expansion behavior of lithium zinc silicate sealing glass, Ceram. Int. 42 (2016) 11650–11653.
[9] E. Demirkesen, Z.E. Erkmen, N. Yildiz, Effect of Al_2O_3 additions on the thermal expansion behavior of a $Li_2O–ZnO–SiO_2$ glass–ceramic, J. Am. Ceram. Soc. 82 (1999) 3619–3621.

[10] E. Demirkesen, E. Maytalman, Effect of Al_2O_3 additions on the crystallization behavior and bending strength of a Li_2O–ZnO–SiO_2 glass–ceramic, Ceram. Int. 27 (2001) 99–104.
[11] E. Demirkesen, G. Göller, Effect of Al_2O_3 additions on the acid durability of a Li_2O–ZnO–SiO_2 glass and its glass–ceramic, Ceram. Int. 29 (2003) 463–469.
[12] X. Zheng, G. Wen, L. Song, X.X. Huang, Effects of P_2O_5 and heat treatment on crystallization and microstructure in lithium disilicate glass ceramics, Acta Mater. 56 (2008) 549–558.
[13] Z. Xiao, X. Sun, K. Liu, W. Luo, Y. Wang, M. Luo, R. Han, Y. Liu, Crystallization behaviors, thermo-physical properties and seal application of Li_2O–ZnO–MgO–SiO_2 glass–ceramics, J. Alloys Compd. 657 (2016) 231–236.
[14] W. Liu, Z. Luo, X. Hu, A. Lu, Effect of MgO addition on crystallization and properties of Li_2O–ZnO–SiO_2 glass–ceramics seals for copper, Thermochim. Acta 584 (2014) 45–50.
[15] S.M. Salman, H. Darwish, E.A. Mahdy, The influence of Al_2O_3, MgO and ZnO on the crystallization characteristics and properties of lithium calcium silicate glasses and glass–ceramics, Mater. Chem. Phys. 112 (2008) 945–953.
[16] S.M. Salman, S.N. Salama, E.A. Mahdy, Crystallization and thermo-mechanical properties of Li_2O–ZnO–CaO–SiO_2 glass–ceramics with In_2O_3 and Fe_2O_3 additives, Process. Appl. Ceram. 9 (2015) 215–223.
[17] I.M. Stewart, G.J.P. Buchi, Phase relationship in the system Li_2O–ZnO–SiO_2, Trans. Br. Ceram. Soc. 61 (1962) 615–622.
[18] S.N. Salama, S.M. Salman, Chemical stability of some manganese glass–ceramics, Mater. Chem. Phys. 37 (1994) 338–343.
[19] H.A. Abo-Mosallam, S.N. Salama, S.M. Salman, Contribution of gallium oxide content to the crystallization characteristics and chemical stability of sodium phlogopite glasses, Ceram. Int. 40 (2014) 8037–8044.
[20] M. Karabulut, B. Yuce, O. Bozdogan, H. Ertap, G.M. Mammadov, Effect of boron addition on the structure and properties of iron phosphate glasses, J. Non-Cryst. Solids 357 (2011) 1455–1462.
[21] F. Wang, Q. Liao, K. Chen, S. Pan, M. Lu, Glass formation and FTIR spectra of CeO_2-doped 36Fe_2O_3–10B_2O_3–54P_2O_5 glasses, J. Non-Cryst. Solids 409 (2015) 76–82.
[22] H. Ren, Y. Yue, C. Ye, L. Guo, J. Lei, NMR study of crystallization in MgO–CaO–SiO_2–P_2O_5 glass ceramics, Chem. Phys. Lett. 292 (1998) 317–322.
[23] C. Lara, M.J. Pascual, M.O. Prado, A. Durán, Sintering of glasses in the system RO–Al_2O_3–BaO–SiO_2 (R = Ca, Mg, Zn) studied by hot-stage microscopy, Solid State Ionics 170 (2004) 201–208.
[24] H.A. Abo-Mosallam, S.N. Salama, S.M. Salman, Formulation and characterization of glass–ceramics based on $Na_2Ca_2Si_3O_9$–$Ca_5(PO_4)_3F$–Mg_2SiO_4-system in relation to their biological activity, J. Mater. Sci. Mater. Med. 20 (2009) 2385–2394.
[25] T.F. Barth, Theoretical Petrology, 2nd ed., Wiley, New York, 1962.
[26] S.M. Salman, A.A. Omar, S.N. Salama, Solid solution phases from thermally crystallized Li_2O–MgO–Al_2O_3–SiO_2 glasses, Mater. Chem. Phys. 11 (1984) 145–160.
[27] J. Zhang, Y. Zhu, J. Li, M. Zhu, C. Tao, N. Hanagata, Preparation and characterization of multifunctional magnetic mesoporous calcium silicate materials, Sci. Technol. Adv. Mater. 14 (2013) 1–10.
[28] Z. Cui, G. Jia, D. Deng, Y. Hua, S. Zhao, L. Huang, H. Wang, H. Ma, S. Xu, Synthesis and luminescence properties of glass ceramics containing $MSiO_3$:Eu2+ (M = Ca, Sr, Ba) phosphors for white LED, J. Lumin. 132 (2012) 153–160.
[29] N. Tangboriboon, S. Pakdeeniti, R. Kunanuruksapong, A. Sirivat, Calcium silicate ($CaSiO_3$) as alternative ionic coagulant and solid lubricant for ceramic molds in natural rubber latex film preparation, Rubber Chem. Technol. 85 (2012) 645–660.
[30] L.C. Ferracin, M.R. Davolos, L.A.O. Nunes, MnO_4^{3-} NIR luminescence in Ba_2SiO_4, J. Lumin. 72–74 (1997) 185–187.
[31] X. Qu, L. Cao, W. Liu, G. Su, C. Xu, P. Wang, Preparation and properties of $CdSiO_3$:Mn^{2+}, Dy^{3+} phosphor, J. Alloys Compd. 494 (2010) 196–198.
[32] W.A. Deer, R.A. Howie, J. Zussman, Introduction to the Rock Forming Minerals, Longman, Harlow, England, 1992, pp. 140–143.
[33] S.S. Yao, L.H. Xue, Y.Y. Li, Y. You, Y.W. Yan, Concentration quenching of Eu^{2+} in a novel blue–green emitting phosphor: $Ba_2ZnSi_2O_7$:Eu^{2+}, Appl. Phys. B 96 (2009) 39–42.
[34] B. Tiwari, A. Dixit, C.G.S. Pillai, S.C. Gadkari, G.P. Kothiyal, Crystallization kinetics and mechanism of strontium zinc silicate glass, J. Am. Ceram. Soc. 95 (2012) 1290–1296.
[35] A.X. Lu, Z.B. Ke, Z.H. Xiao, X.F. Zhang, X.Y. Li, Effect of heat-treatment condition on crystallization behavior and thermal expansion coefficient of Li_2O–ZnO–Al_2O_3–SiO_2–P_2O_5 glass–ceramics, J. Non-Cryst. Solids 353 (2007) 2692–2697.
[36] A. Hu, K. Liang, M. Li, D. Mao, Effect of nucleation temperatures and time on crystallization behavior and properties of Li_2O–Al_2O_3–SiO_2 glasses, Mater. Chem. Phys. 98 (2006) 430–433.
[37] A.R. West, F.P. Glasser, Crystallization of lithium zinc silicates. Part 2. Comparison of the metastable and stable phase relations and the properties of the lithium zinc orthosilicates, J. Mater. Sci. 5 (1970) 676–688.
[38] P.W. McMillan, Glass–Ceramics, Academic Press, London, NY, 1979.
[39] G. Muller, Structure, composition, stability and thermal expansion of high eucryptite and keatite type aluminosilicate, in: H. Bach (Ed.), Low Thermal Expansion Glass–Ceramic, 2nd ed., Springer-Verlag, Berlin, 1995, pp. 13–25.
[40] C. Thieme, M. Schlesier, C. Bocker, G. Buzatto de Souza, C. Rüssel, Thermal expansion of sintered glass ceramics in the system BaO–SrO–ZnO–SiO_2 and its dependence on particle size, Appl. Mater. Interfaces 8 (2016) 20212–20219.
[41] C. Thieme, C. Russel, Thermal expansion behavior of $SrSiO_3$ and Sr_2SiO_4 determined by high-temperature X-ray diffraction and dilatometry, J. Mater. Sci. 50 (2015) 5533–5539.
[42] P. Riello, P. Canton, N. Comelato, S. Polizzi, M. Verità, G. Fagherazzi, H. Hofmeister, S. Hopfe, Nucleation and crystallization behavior of glass–ceramic materials in the Li_2O–Al_2O_3–SiO_2 system of interest for their transparency properties, J. Non-Cryst. Solids 288 (2001) 127–139.
[43] M. Guedes, A.C. Ferro, J.M.F. Ferreira, Nucleation and crystal growth in commercial LAS compositions, J. Eur. Ceram. Soc. 21 (2001) 1187–1194.
[44] J. Christoffersen, M.R. Christoffersen, N. Kolthoff, O. Bärenholdt, Effects of strontium ions on growth and dissolution of hydroxyapatite and on bone mineral detection, Bone 20 (1997) 47.